Key words 3D-SSP · Alzheimer's disease · SPECT · PET

Introduction

For the clinical diagnosis of Alzheimer's disease (AD), regional glucose metabolism and cerebral blood flow (rCBF) are measured by positron emission tomography (PET) and single photon emission computed tomography (SPECT), respectively. Several studies have reported that changes in the regional glucose metabolism or rCBF are useful for the diagnosis of AD.[1–8]

Recent computational advances have improved the detection of regional metabolic and perfusion change using three-dimensional stereotactic surface projections (3D-SSP) or statistical parametric mapping (SPM) for the clinical diagnosis.[9–16] These two methods use PET and SPECT to analyze an individual brain in comparison with a standard brain, after stereotactic normalization, pixel by pixel or voxel by voxel. Ishii et al. showed that the fully automatic diagnostic system, using 3D-SSP, was able to perform at a diagnostic level similar to that of the visual inspection of conventional axial images by experts using the glucose analog 2-[^{18}F]-fluoro-2-deoxy-D-glucose (FDG)-PET.[17] Imabayashi et al. showed that the ability of 3D-SSP to discriminate early AD patients from control subjects was superior to that of visual inspection.[14] Tang et al. reported that the addition of 3D-SSP to the transaxial section display of SPECT improved the reproducibility and the diagnostic performance of AD.[12]

In terms of a comparison between PET and SPECT, it is apparent that PET has the advantage of greater sensitivity and greater spatial resolution. SPECT is the most widely available modality for functional neuroimaging techniques to evaluate dementia. Because the availability of PET is limited, PET is not used as often as SPECT clinically. Recently, the use of 3D-SSP or SPM has enabled the diagnosis of AD with greater accuracy.

Few reports have made a direct comparison of the diagnostic ability between PET and SPECT using statistical brain mapping methods in the same patients. Therefore, the purpose of the present study is to compare the ability to discriminate an AD pattern from healthy subjects using a 3D-SSP analysis of FDG-PET and *N*-isopropyl-*p*-^{123}I iodoamphetamine (IMP)-SPECT with visual interpretation by four expert physicians.

Methods

Subjects

Informed consent was obtained from all subjects prior to their participation in this study, which was approved by the ethics committee at our institution. FDG-PET and IMP-SPECT were performed on 14 patients (6 men, 8 women) within at least 3 months. The mean age was 70.1 ± 8.5 years. These patients were diagnosed as having probable AD according to the National Institute of Neurological and Communicative Disorders and Stroke (NINCDS) and the Alzheimer's disease and Related Disorders Association (ADRDA) criteria. The mean score of the Mini-Mental State Examination (MMSE) for these patients was 18.8 ± 4.3. For the FDG-PET study, seven subjects (four men, three women; mean age 61.2 years) participated as normal controls (NC), and for the IMP-SPECT study, nine subjects (two men, seven women; mean age 70.1 years) participated as normal controls.

FDG-PET

An ECAT EXACT HR 47 PET camera (Siemens/CTI, Germany) was used, and imaging was performed using two-dimensional acquisition at 60 min after intravenous administration of ^{18}F-FDG (370 MBq). Before FDG-PET scanning, the subjects rested in a supine position with eyes closed in a quiet room. The collected data were reconstructed into 128 × 128 pixel image matrices. Tissue attenuation of annihilation photons was corrected by transmission scans using rotating ^{68}Ge/^{68}Ga line sources. The in-plane spatial resolution was 4.0 × 3.9 mm in full-width at half-maximum (FWHM). The patient fasted for at least 6 h prior to the examination. Normal glucose levels were confirmed prior to the PET scan.

IMP-SPECT

A total of 222 MBq (6 mCi) of ^{123}I-IMP (Nihon Mediphysics, Hyogo, Japan) was injected into an antecubital vein while the subjects rested in a supine position with eyes closed in a quiet room. A single blood sample was obtained from the brachial artery between 9 and 10 min after the ^{123}I-IMP administration. SPECT scanning was carried out between 15 and 45 minutes after injection using a two-head rotating GCA 7200DI gamma camera (Toshiba, Tokyo, Japan) fitted with low-energy, high-resolution collimators. The data were acquired in 128 × 128 matrices through a 18° rotation at an angle interval of 4°. The projection data were prefiltered through a Butterworth filter and reconstructed using a Ramp back-

Table 1. Normal database of FDG-PET and IMP-SPECT

Method	No.	Sex (M/F)	Age
FDG-PET	37	23/11	59.0
IMP-SPECT	18	7/F	69.9

FDG-PET, 2-[^{18}F]-fluoro-2-deoxy-D-glucose positron emission tomography; IMP-SPECT, *N*-isopropyl-*p*-^{123}I iodoamphetamine single photon emission computed tomography

projection filter. Chang's attenuation correction and scattering correction using the triple energy window method were applied to the reconstructed images. The in-plane spatial resolution was 11.1 mm in FWHM. The final image slices were set parallel to the orbitomeatal line and were obtained at an interval of 3.44 mm through the entire brain. The rCBF images were quantitated according to the IMP-ARG method.[18]

Statistical images (3D-SSP)

The original FDG-PET and IMP-SPECT data were analyzed by an iSSP (SSP; Nihon Mediphysics) program, which was modified based on the NEUROSTAT program (Dr. Minoshima, Department of Radiology and Bioengineering, University of Washington, Seattle, WA, USA). After rotation and centering of the data set, the original data were realigned to the bicommissural line (AC-PC) and transformed into a stereotactic standard Talairach space. The cortical peak activity was projected onto the brain surface, and the peak value was projected back and assigned to the originating surface pixel. The extracted data sets were displayed on eight different angles, including the lateral, medial, superior, inferior, anterior, and posterior views. With the 3D-SSP programs in NEUROSTAT, the pixel values were normalized to the whole brain, thalamus, pons, and cerebellum (Fig. 1). The pixel values of an individual's image were compared with a normal database that originated at our institution (Table 1). The normal database was built as follows: 18 normal subjects (7 men, 11 women; mean age 69.9 years) for IMP-SPECT and 37 normal subjects (23 men, 14 women; mean age 59.0 years) for FDG-PET.

Statistical analysis/visual interpretation

Four nuclear medicine physicians randomly interpreted FDG-PET images of 14 AD patients and 7 NCs and IMP-SPECT images of 9 NCs. The interpretation of each image was performed at separate sessions, respectively. The statistical analyses were conducted using the following procedure. Two areas of the brain, the posterior cingulate gyri/precunei and parietotemporal region in each image (which were determined as characteristic for AD in advance of the study) were evaluated.[9] The degree of reduction in glucose metabolism or rCBF were interpreted, and a score of 5 was assigned if the change was considered "apparent decrease," which is characteristic of AD. Accordingly, scores of 4 to 1 were assigned to the changes that were considered "probable decrease," "unclear," "probable not a decrease," and "apparently not a decrease," respectively. Then, the reliability was evaluated using five steps similar to the regional evaluation.

When laterality was observed in a visual interpretation, the evaluation of a regional change was performed as follows. The scores assigned to the right and left sides (of the brain) of FDG-PET were compared for each side of the brain, and the higher score was recorded as the case's FDG-PET score for the specific area of the brain. The side of the higher FDG-PET score was considered a regional finding, and the IMP-SPECT score of the same side was recorded as the case's IMP-SPECT score. If the right- and left-side FDG-PET scores were the same, the higher score in IMP-SPECT was recorded as the regional finding. In fact, there were no discrepancies between the FDG-PET scores and the IMP-SPECT images in terms of laterality.

Second, the ratings of four readers were pooled for each area and for each image. The ROC analysis was performed for the graphics presentation, and the area under the curve was calculated to express the diagnostic accuracy of each image and each area numerically. Confidence intervals (CIs) of the AUC were used to test the difference in overall diagnostic accuracy between the images, the upper and lower limits of which were calculated either by adding or subtracting the standard error of the AUC times 1.96 for 95% CI and 1.65 for 90% CI. Because our primary interest lies in the difference in the diagnostic ability of FDG-PET from IMP-SPECT, we did not compare the difference in the AUC between the areas of the brain and did not take multiplicity in comparison into account. $P < 0.05$ was considered statistically significant. The statistical analyses were conducted using SPSS for Windows.

Correlation between FDG-PET and IMP-SPECT

To assess the agreement between two modalities, ROIs were set in the posterior cingulate gyri/precunei and parietotemporal region on 3D-SSP images, of which the pixel values were normalized to the whole brain bilaterally (Fig. 2). Then the mean Z-values of the right and left hemisphere were summed and used for analysis. We calculated kappa (κ) statistics, the proportion of concordance, and the Spearman's correlation coefficients of

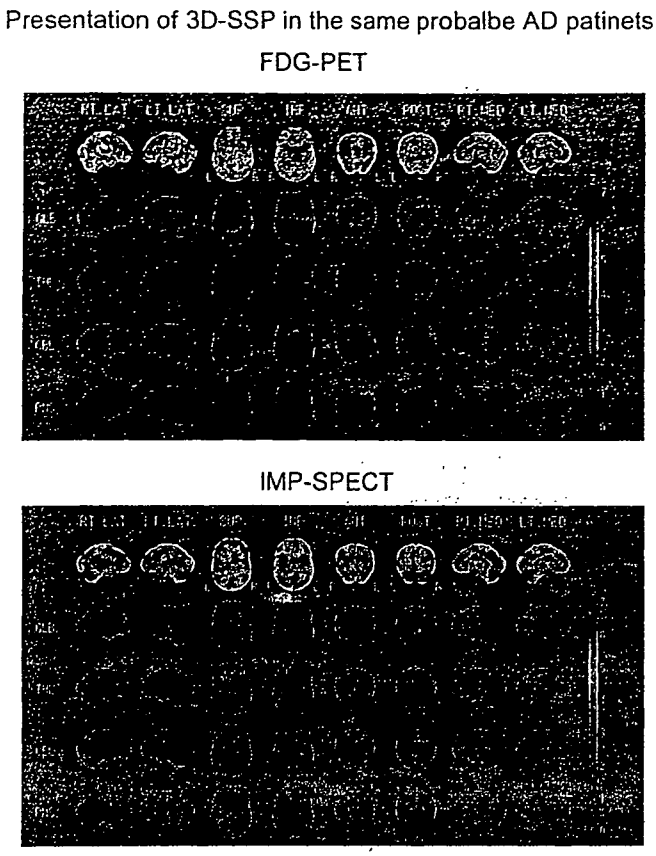

Fig. 1. Z-score images of three-dimensional stereotactic surface projections (3D-SSP) are shown from a representative Alzheimer's disease (AD) patient. These images demonstrate a decrease in the glucose metabolism and regional cerebral blood flow (rCBF). *Upper panel*: 2-[^{18}F]-Fluoro-2-deoxy-D-glucose positron emission tomography (FDG-PET). *Lower panel*: *N*-Isopropyl-*p*-^{123}I iodoamphetamine single photon emission computed tomography (IMP-SPECT). The extracted data sets are displayed on eight different angles, including the lateral (*RT LAT*, *LT LAT*), medial (*RT MED*, *LT MED*), superior (*SUP*), inferior (*INF*), anterior (*ANT*), and posterior (*POST*) views. With the 3D-SSP programs in NEUROSTAT, the pixel values are normalized to the whole brain (*GLB*), thalamus (*THL*), cerebellum (*CBL*), and pons (*PNS*)

Z-values in each area (the posterior cingulate gyri/precunei and parietotemporal region). For assessing κ statistics and the proportion of concordance, Z-values were first categorized according to their quartiles. Then the lowest quartile was considered as the "decrease" category. The κ statistic is defined as the agreement beyond chance divided by the amount of agreement possible by chance. As in most studies, $\kappa > 0.75$ was taken to represent excellent agreement beyond chance, 0.40–0.75 to mean fair agreement, and <0.40 to mean poor agreement.[19]

Results

Figure 3 shows the results of the clinical diagnosis of AD by 3D-SSP. The AUC of FDG-PET was 0.952 ± 0.023, and that of IMP-SPECT was 0.935 ± 0.026. There was no significant difference between FDG-PET and IMP-SPECT. Table 2 shows the results of each interpreter and the sum as the diagnosis ability. The sensitivity and specificity of each modality were 86%, and 97% for FDG-PET and 70%, and 100% for IMP-SPECT, respectively (Table 3).

Table 2. Results of visual inspection of 3D-SSP by each interpreter

	FDG-PET		IMP-SPECT	
Interpreter	AUC	SE	AUC	SE
A	0.939	0.057	0.976	0.026
B	0.954	0.047	0.96	0.041
C	0.888	0.074	0.821	0.091
D	0.995	0.01	1	0
Sum	0.952	0.023	0.935	0.026

3D-SSP, three-dimensional stereotactic surface projections; AUC, area under the curve; SE, standard error

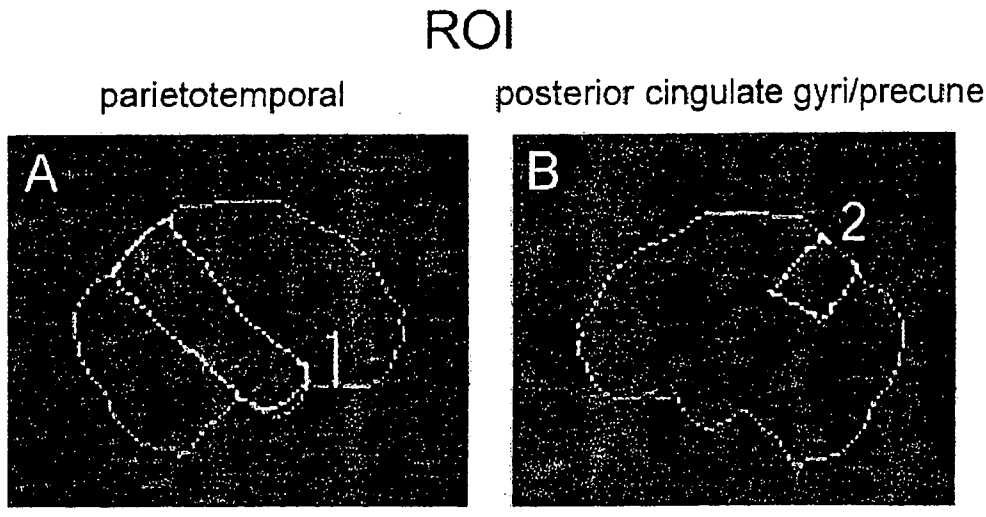

Fig. 2. Regions of interest (ROI) were set in the posterior cingulate gyri/precunei (B) and parietotemporal region (A) on 3D-SSP images of FDG-PET, in which the pixel values were normalized to the whole brain bilaterally

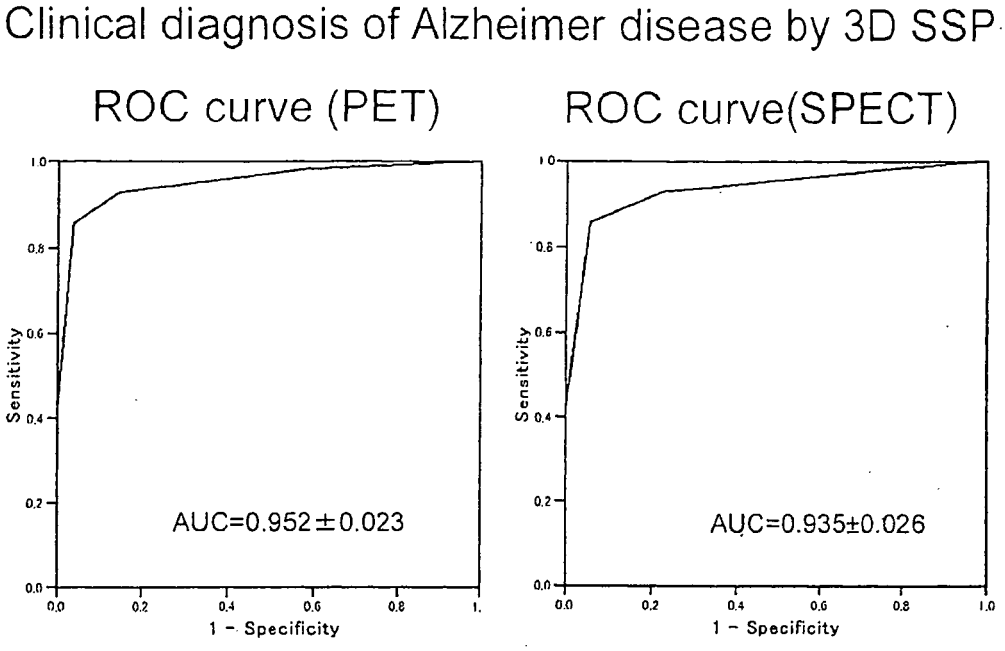

Fig. 3. Receiver operating characteristic (ROC) curves for clinical diagnosis of AD with visual inspection by experts. There was no significant difference between PET and SPECT. *AUC*, area under the curve

Table 3. Results of visual inspection of 3D-SSP by each interpreter: sensitivity and specificity

Interpreter	FDG-PET		IMP-SPECT	
	Sensitivity (%)	Specificity (%)	Sensitivity (%)	Specificity (%)
A	93	100	64	100
B	79	100	79	100
C	86	86	64	100
D	86	100	71	100
Sum	344	386	278	400
Average	86	97	70	100

Figure 4 shows the regional evaluation of the posterior cingulate gyri/precuneus and the parietotemporal region. The AUC of FDG-PET was 0.935 ± 0.028, and that of IMP-SPECT was 0.807 ± 0.046 in the posterior cingulate gyri/precuneus. A significant difference between FDG-PET and IMP-SPECT was observed ($P < 0.05$). The AUC of FDG-PET was 0.871 ± 0.038, and that of IMP-SPECT was 0.802 ± 0.046 in the parietotemporal region. There was no significant difference between FDG-PET and IMP-SPECT detected for this region.

Interrater agreement among four nuclear medicine physicians was evaluated by intraclass correlation coefficient with the Spearman-Brown correction. For both PET and SPECT, the agreement in the ratings among four raters were high: PET 0.94, SPECT 0.96.

There was a high correlation of Z-values between FDG-PET and IMP-SPECT in the parietotemporal region (Spearman's $r = 0.82$, $P < 0.001$). The correlation of the two modalities in the posterior cingulate gyri/precunei region was lower than that in the parietotemporal region (Spearman's $r = 0.63$, $P < 0.016$). In terms of the proportion of concordance and κ statistics, there was a perfect agreement in the parietotemporal region (both 1.0, $P < 0.001$). The proportion of concordance in the posterior cingulate gyri/precunei region was comparable (0.71), but agreement beyond chance evaluated by the κ statistics was poor and not significantly greater than zero (0.15, $P = 0.57$).

Discussion

Voxel-based statistical mapping methods, such as 3D-SSP and SPM, have been reported to be useful when delineating AD individuals from normal subjects.[9–16,20,21] Honda et al showed that 3D-SSP enhanced the specificity of SPECT inspection by nuclear medicine physicians

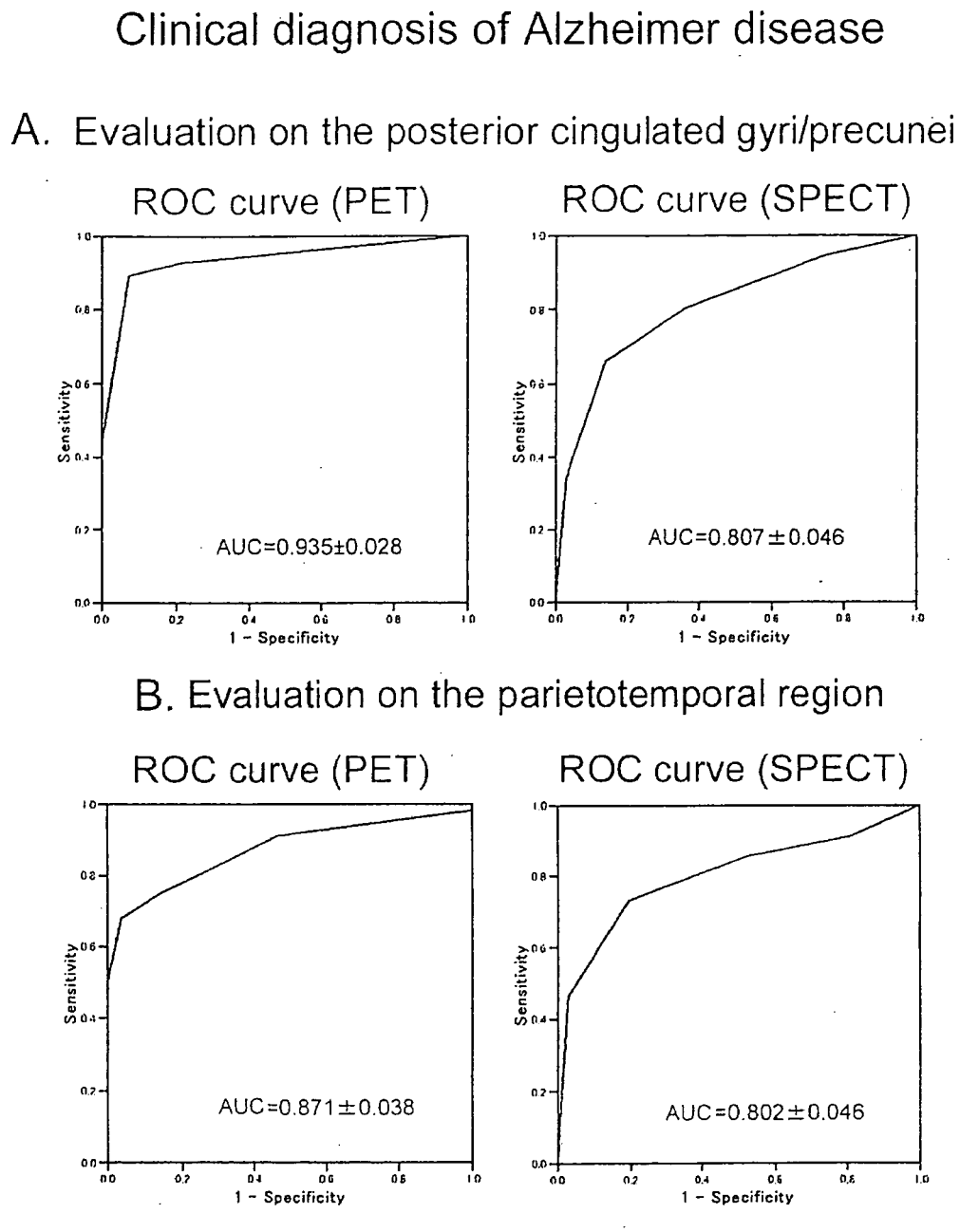

Fig. 4. ROCs for clinical diagnosis of AD with visual inspection of the posterior cingulated gyri/precuneus (A) and the parietotemporal region (B). For evaluation of the posterior cingulated gyri/precuneus, PET is significantly superior to SPECT

and the performance of the automated diagnosis, when focusing on the posterior cingulate gyri and precunei, exceeded that of the physicians when evaluating SPECT with and without 3D-SSP.[11] These reports showed that voxel-based statistical mapping methods may add useful information when diagnosing AD. The usefulness of such statistical methods has become clear, and these methods are used frequently clinically.

A few studies have compared FDG-PET and rCBF SPECT directly in terms of diagnosing AD. Mielke et al. reported that both PET and SPECT are able to distinguish AD patients from controls. On the other hand, for differentiation between AD and vascular dementia (VD), PET was shown to be superior to SPECT.[22] Messa et al. reported that both PET and SPECT were able to detect characteristic temporoparietal abnormalities in probable AD, whereas for the evaluation for other associative areas PET was superior to SPECT.[23] Silverman reported that higher diagnostic accuracy was obtained with PET than with SPECT, and the increased accuracy was estimated to be approximately 15%–20%.[24] Herholz et al. reported that correspondence between PET and SPECT was limited to the main finding of temporoparietal and posterior cingulate functional impairment in mild to moderate AD using SPM.[25] Although many studies have shown that PET is superior to SPECT in terms of diag-

nosing AD, it seems that a decisive difference has not been determined concerning the diagnostic ability of PET and SPECT as far as the posterior cingulate gyri/precuneus and the parietotemporal region are concerned, which are the characteristic regions for AD.

In the present study, our purpose was to compare directly the diagnostic ability of FDG-PET and IMP-SPECT using 3D-SSP and focusing on as the posterior cingulate gyri/precuneus and the parietotemporal region. Our results show that there was no significant difference between FDG-PET and IMP-SPECT in terms of diagnosing AD using 3D-SSP. However, there was a tendency that FDG-PET was slightly superior to IMP-SPECT, especially when evaluating the posterior cingulate gyri/precuneus. These results are consistent with those of previous studies and our clinical experience. We considered two possibilities to explain the findings. First, a possible reason why FDG-PET is superior to IMP-SPECT is that the metabolic change due to degeneration might slightly proceed to a decrease in rCBF. Second, PET has the advantage of greater sensitivity and greater spatial resolution. Both possibilities were plausible.

We found that there was a high correlation of Z-values between FDG-PET and IMP-SPECT in the parietotemporal region; in contrast, there was not a good correlation in the posterior cingulate gyri/precunei region. These results showed that there was the difference between the glucose metabolic and rCBF changes in the posterior cingulate gyri/precunei region. We considered two possibilities regarding this problem. First, coupling the glucose metabolic change and rCBF change might depend on the degree of the degeneration. Therefore, in the posterior cingulate gyri/precunei region, because the degenerative change is slight, the change in glucose metabolism might be greater than that of the rCBF change. Second, distributions of the glucose metabolism and rCBF were not the same in every area of the brain. Sakamoto and Ishii showed that there are great glucose metabolic and rCBF differences between the medial temporal lobe, the cerebellum, and other brain regions in the normal human brain.[26] If there was a difference between the glucose metabolism and rCBF in the posterior cingulate gyri/precunei region, it was not impossible to understand this result. To evaluate the finding in the posterior cingulate gyri/precunei region, further studies are needed from a radiological and/or pathological approach.

There are three restrictions to the present study. First, the normal controls and normal database differed, respectively, for FDG-PET and IMP-SPECT. Ideally, for each examination, the normal controls and database should be the same. However, prescribing nuclear medicine to healthy subjects twice in a short time is difficult. Second, in the present study, we analyzed only moderately affected AD patients. Recently, Dobert et al. evaluated the diagnostic potential of FDG-PET and SPECT in terms of early detection and the differential diagnosis of early dementia in the same patients and showed that PET was the superior imaging method, especially for detecting early AD or mixed-type dementia.[27] If we analyze early or mild AD, the results may change. Third, owing to a relatively small number of subjects, the statistical power might have been limited in the present study. In an illustrative example dataset where a total of about 160 subjects were studied in which the correlation of the underlying bivariate binormal distribution is 0.75, statistical power to detect a 0.10 difference in the AUC of the two modalities was estimated as 0.75.[28] In the present study, a total of about 90 subjects were studied where the AUC difference of more than 0.1 had been expected, and the statistical power of the analysis would have been retained to a similar degree. Thus, the present finding of no difference could be interpreted as relevant. Ideally, further studies with larger sample sizes are needed to examine whether these two modalities are really equivalent in diagnosing AD given that we did not observe a statistically significant difference in the AUC between FDG-PET and IMP-SPECT.

Using 3D-SSP, our results show that FDG-PET and IMP-SPECT have similar diagnostic ability in moderately affected AD patients. However, there was the tendency that the ability of FDG-PET to detect probable AD was superior to that of IMP-SPECT. Specifically, for regional glucose metabolism or cerebral blood flow analysis of the posterior cingulate gyri/precuneus, PET was significantly superior to SPECT.

References

1. Duara R, Grady C, Haxby J, Sundaram M, Cutler NR, Heston L, Moore A, et al. Positron emission tomography in Alzheimer's disease. Neurology 1986;3:879–87.
2. Heiss WD, Szelies B, Kessler J, Herholz K. Abnormalities of energy metabolism in Alzheimer's disease studied with PET. Ann N Y Acad Sci 1991;640:65–71.
3. Silverman DH, Small GW, Chang CY, Lu CS, Kung De Aburto MA, Chen W, et al. Positron emission tomography in evaluation of dementia: regional brain metabolism and long-term outcome. JAMA 2001;286:2120–7.
4. Bradley KM, O'Sullivan VT, Soper ND, Nagy Z, King EM, Smith AD, et al. Cerebral perfusion SPECT correlated with Braak pathological stage in Alzheimer's disease. Brain 2002; 125:1772–81.
5. Ishii K. Clinical application of positron emission tomography for diagnosis of dementia. Ann Nucl Med 2002;16:515–25.
6. Herholz K, Salmon E, Perani D, Baron JC, Holthoff V, Frolich L, et al. Discrimination between Alzheimer dementia and controls by automated analysis of multicenter FDG PET. Neuroimage 2002;17:302–16.

7. Herholz K. PET studies in dementia. Ann Nucl Med 2003;17: 79–89.
8. Hirao K, Ohnishi T, Hirata Y, Yamashita F, Mori T, Moriguchi Y, et al. The prediction of rapid conversion to Alzheimer's disease in mild cognitive impairment using regional cerebral blood flow SPECT. Neuroimage 2005; 28:1014–21.
9. Minoshima S, Frey KA, Koeppe RA, Foster NL, Kuhl DE. A diagnostic approach in Alzheimer's disease using three-dimensional stereotactic surface projections of fluorine-18-FDG PET. J Nucl Med 1995;36:1238–48.
10. Burdette JH, Minoshima S, Vander Borght T, Tran DD, Kuhl DE. Alzheimer disease: improved visual interpretation of PET images by using three-dimensional stereotaxic surface projections. Radiology 1996;198:837–43.
11. Honda N, Machida K, Matsumoto T, Matsuda H, Imabayashi E, Hashimoto J, et al. Three-dimensional stereotactic surface projection of brain perfusion SPECT improves diagnosis of Alzheimer's disease. Ann Nucl Med 2003;17: 641–8.
12. Tang BN, Minoshima S, George J, Robert A, Swine C, Laloux P, et al. Diagnosis of suspected Alzheimer's disease is improved by automated analysis of regional cerebral blood flow. Eur J Nucl Med Mol Imaging 2004;31:1487–94.
13. Kaneko K, Kuwabara Y, Sasaki M, Ogomori K, Ichimiya A, Koga H, et al. Posterior cingulate hypoperfusion in Alzheimer's disease, senile dementia of Alzheimer type, and other dementias evaluated by three-dimensional stereotactic surface projections using Tc-99m HMPAO SPECT. Clin Nucl Med 2004;29:362–6.
14. Imabayashi E, Matsuda H, Asada T, Ohnishi T, Sakamoto S, Nakano S, et al. Superiority of 3-dimensional stereotactic surface projection analysis over visual inspection in discrimination of patients with very early Alzheimer's disease from controls using brain perfusion SPECT. J Nucl Med 2004; 45:1450–7.
15. Kemp PM, Hoffmann SA, Holmes C, Bolt L, Ward T, Holmes RB, et al. The contribution of statistical parametric mapping in the assessment of precuneal and medial temporal lobe perfusion by ^{99m}Tc-HMPAO SPECT in mild Alzheimer's and Lewy body dementia. Nucl Med Commun 2005;26: 1099–106.
16. Kim EJ, Cho SS, Jeong Y, Park KC, Kang SJ, Kang E, et al. Glucose metabolism in early onset versus late onset Alzheimer's disease: an SPM analysis of 120 patients. Brain 2005;128:1790–801.
17. Ishii K, Kono AK, Sasaki H, Miyamoto N, Fukuda T, Sakamoto S, et al. Fully automatic diagnostic system for early- and late-onset mild Alzheimer's disease using FDG PET and 3D-SSP. Eur J Nucl Med Mol Imaging 2006;10:1–9.
18. Iida H, Itoh H, Nakazawa M, Hatazawa J, Nishimura H, Onishi Y, et al. Quantitative mapping of regional cerebral blood flow using iodine-123-IMP and SPECT. J Nucl Med 1994;35:2019–30.
19. Fleiss J. The measurement of interrater agreement. In: Statistical methods for rates and proportions. 2nd edition. New York: Wiley; 1981. p. 212–36.
20. Dougall NJ, Bruggink S, Ebmeier KP. Systematic review of the diagnostic accuracy of ^{99m}Tc-HMPAO-SPECT in dementia. Am J Geriatr Psychiatry 2004;12:554–70.
21. Huang C, Wahlund LO, Almkvist O, Elehu D, Svensson L, Jonsson T, et al. Voxel- and VOI-based analysis of SPECT CBF in relation to clinical and psychological heterogeneity of mild cognitive impairment. Neuroimage 2003;19:1137–44.
22. Mielke R, Pietrzyk U, Jacobs A, Fink GR, Ichimiya A, Kessler J, et al. HMPAO SPET and FDG PET in Alzheimer's disease and vascular dementia: comparison of perfusion and metabolic pattern. Eur J Nucl Med 1994;21:1052–60.
23. Messa C, Perani D, Lucignani G, Zenorini A, Zito F, Rizzo G, et al. High-resolution technetium-99m-HMPAO SPECT in patients with probable Alzheimer's disease: comparison with fluorine-18-FDG PET. J Nucl Med 1994;35:210–6.
24. Silverman DH. Brain ^{18}F-FDG PET in the diagnosis of neurodegenerative dementias: comparison with perfusion SPECT and with clinical evaluations lacking nuclear imaging. J Nucl Med 2004;45:594–607.
25. Herholz K, Schopphoff H, Schmidt M, Mielke R, Eschner W, Scheidhauer K, et al. Direct comparison of spatially normalized PET and SPECT scans in Alzheimer's disease. J Nucl Med 2002;43:21–6.
26. Sakamoto S, Ishii K. Low cerebral glucose extraction rates in the human medial temporal cortex and cerebellum. J Neurol Sci 2000;172:41–8.
27. Dobert N, Pantel J, Frolich L, Hamscho N, Menzel C, Grunwald F. Diagnostic value of FDG-PET and HMPAO-SPET in patients with mild dementia and mild cognitive impairment: metabolic index and perfusion index. Dement Geriatr Cogn Disord 2005;20:63–70.
28. Zhou XH, Obuchowski NA, McClish DK. Statistical methods in diagnostic medicine. New York: Wiley; 2002.

PET/SPECTによるMCIから初期認知症への進行評価

加藤隆司，伊藤健吾

抄 録

MCI（Mild Cognitive Impairment，軽度認知障害）は，正常と認知症との境界領域の認知機能の状態を表す概念である．MCIは，将来アルツハイマー病（AD）へ移行する群を高率に含む．移行群では，MCIの段階でAD的なパターンで脳血流/糖代謝が低下している．移行群と非移行群を分ける特徴的低下部位はinferior parietal cortexである．このような低下を検出するには，統計学的画像解析の手法が有用である．現在MCIを対象に，画像検査の有効性を検証する大規模臨床研究が日本，ヨーロッパ，アメリカ合衆国，オーストラリアで行われている．

Key words：MCI，軽度認知障害，アルツハイマー病，SPECT，PET

老年精神医学雑誌 18：834-840，2007

1 MCIという概念

MCI（Mild Cognitive Impairment，軽度認知障害）は，正常（高齢者）と認知症の境界領域を表す認知機能の状態の概念として，近年よく用いられるようになった用語である．これまでも，記憶機能の低下に着目して正常と認知症の境界を定義づける概念はほかにあったが，1999年にPetersenが新しく提唱した概念MCI[9]は，アルツハイマー病（Alzheimer's disease；AD）の早期診断，早期治療を目指す臨床研究を進めるうえでの中心的枠組みを提供するに至っている．元来この境界領域は，正常加齢の延長線上に位置づける考え方と，認知症の前駆的状態と位置づける考え方があった．PetersenのMCIは後者の考え方，つまりMCIは進行性の神経疾患の一中間的状態であり，将来認知症に移行していくという考えに基づいている．

表1[6]に示すように，MCIはsubtypeからなる．単一の高次機能領域の障害か複数の高次機能領域の障害かによりsingle domainかmultiple domainに，健忘を示すか記銘力以外の高次脳機能が障害されているかによりamnestic typeかnon-amnestic typeに分ける．現在提唱されている操作的診断基準に基づいて診断されるMCIは単一のものではなく，複数の疾患（病態）を含むと考えられている．病因論的には，アルツハイマー病（AD），レビー小体型認知症（dementia with Lewy bodies；DLB），前頭側頭葉変性症（frontotemporal lobar degeneration；FTLD〈FTD〉）などの変性性認知症，脳血管性認知症（vascular dementia；VaD）などの脳血管障害性病変，抑うつ（depression）などの精神神経学的病態，外傷性変化（trauma），正常加齢などが挙げられる．

Takashi Kato, Kengo Ito：国立長寿医療センター長寿脳科学研究部
〒474-8522 愛知県大府市森岡町源吾36-3

表1　MCIのsubtype

			Etiology				
			Degenerative	Vascular	Psychiatric	Trauma	Aging
Clinical classification	Amnestic MCI	Single domain	AD		Depression		
		Multiple domain	AD	VaD	Depression		
	Non-amnestic MCI	Single domain	FTD				
		Multiple domain	DLB	VaD			

MCI；Mild Cognitive Impairment，AD；アルツハイマー病，FTD；前頭側頭型認知症，DLB；レビー小体型認知症，VaD；脳血管性認知症
(ADNI protocol(03.02.2005) より引用，一部改変)

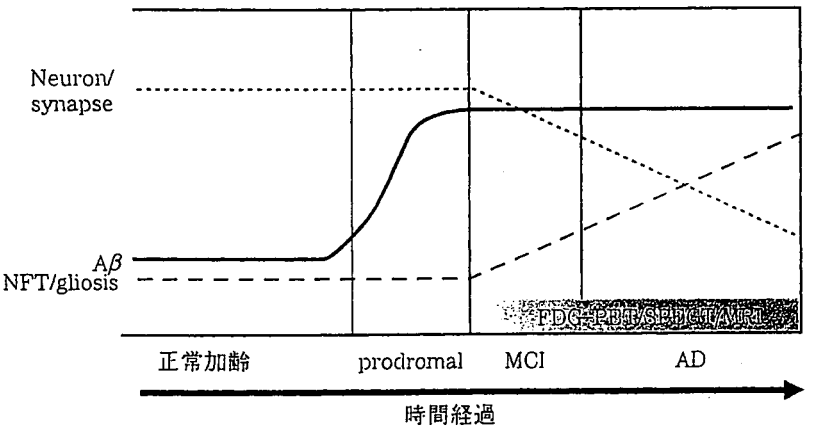

AD；アルツハイマー病，MCI；Mild Cognitive Impairment，NFT；神経原線維変化，Aβ；アミロイドβタンパク
(Ingelsson M, Fukumoto H, Newell KL, Growdon JH, et al.: Early Abeta accumulation and progressive synaptic loss, gliosis, and tangle formation in AD brain. *Neurology*, 62：925-931, 2004 より一部改変)

図1　アルツハイマー病変の時間的進行

2 アルツハイマー病の病理進行からみたMCI

MCIに関して，これまで最も精力的に行われてきたのが，ADに移行する群を，神経心理学的あるいは画像などの検査手段を用いて検出する研究である．ADの病理学的あるいは症候学的進行という観点からは，MCIは図1[7]のように位置づけられる．ADの病理変化の基本は，アミロイドβタンパクの脳内沈着である．図1では，アミロイドβタンパクの沈着が始まる前駆期（prodromal）が想定されている．この前駆期では，神経細胞体あるいはシナプスに変化は起こらず，症候は現れない．続いて，細胞体/シナプスが減少しはじめ，症候が現れるMCI期に進む．アミロイドβタンパクの沈着はほぼ飽和しており，新たに神経原線維変化やグリオーシスが出現しはじめる．ここからさらに病理変化が進行して神経脱落が進むと，認知症（AD）と診断されるレベルに達する．

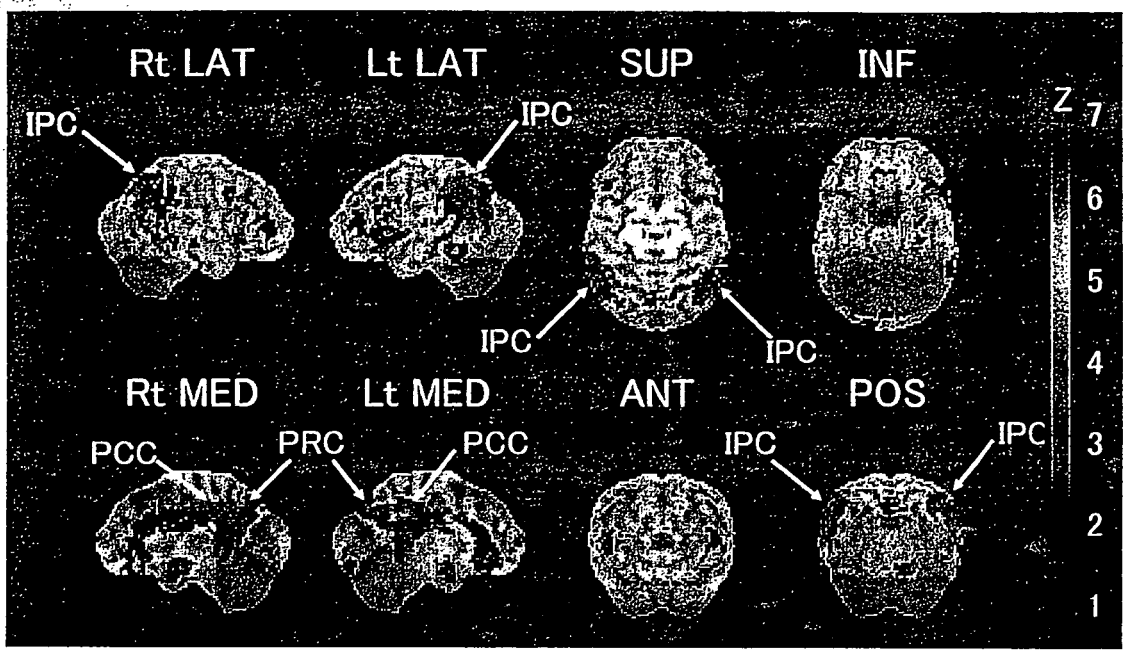

IPC ; inferior parietal cortex, PCC ; posterior cingulate cortex, PRC ; precuneus, LAT ; lateral view, MED ; medial view, SUP ; superior view, INF ; inferior view, ANT ; anterior view, POS ; posterior view, Rt ; right, Lt ; left
IPC, PCC, PRC に糖代謝低下が認められる.

図 2　AD converter の MCI 時点と健常対照群の脳糖代謝 PET 群間比較の Z スコア画像（3D-SSP で MRI 上に表示）

4 年間にわたる研究[9]によると，amnestic MCI と診断された群では年 12% ずつ AD へ移行した．これに対して，正常群での AD への移行率は，年 1 ～ 2% ずつである，とされている．MCI は heterogeneous な患者群であるが，このなかには症例 AD に移行する患者が高率で含まれているといってよい．AD へ移行する MCI（converter）においては，AD の神経病理学的変化を反映した神経活動の低下が生じているはずであり，そのような神経活動の変化を，[I-123] IMP，[Tc-99m] HM-PAO，[Tc-99m] ECD による脳血流 SPECT（single photon emission computed tomography），[F-18] FDG による脳糖代謝 PET（positron emission tomography）で検出する研究が行われてきた．

脳血流，脳糖代謝ともに，その局所のシナプス領域における神経活動を反映しているといわれている．個々の患者のある一時間断面においては，その疾患を特徴づける臨床症状がすべて現れているとは限らない．そのため，脳内に生じている病態をとらえる脳血流 SPECT/脳糖代謝 PET のほうが，診断的価値が高いことが期待されている．

3 AD 移行の surrogate marker

MCI という heterogeneous な集団（患者群）から，AD へ移行する群（converter）を予測する特徴的な脳血流 / 糖代謝変化（surrogate marker あるいは predictor）はなにか．

研究報告は複数あるが，対象が MCI といっても細かい部分で inclusion criteria が異なる，経過観察期間が異なる，前向きあるいは後ろ向き，PET と SPECT など，必ずしも同列に取り扱うことはできない．たとえば非移行群（non-converter）といっても，経過観察期間内で移行しなかったというに過ぎない可能性がある．しかし，これまでの研究結果を全体としてみた場合，AD 移行群は MCI の段階で AD 的なパターンで神経活動の低下が生じている（図 2）ことは確かである．とくに inferior parietal cortex（ないし temporopa-

rietal cortex）が，converterとnon-converterを分ける血流/糖代謝低下部位であることは，各報告でおおむね共通している．大脳内側面のposterior cingulate cortexに関しては，converterとnon-converterを分けるpredictorであるという結果と，posterior cingulateよりprecuneusのほうが重要であるとする報告に分かれている．また，付随的な部位として，prefrontal cortex，hippocampal cortex，entorhinal cortexが挙げられている．

固定的な期間で縦断的にMCIからのADへの移行を検討した最初の報告は，Baronのグループによる[3]．18か月という経過観察期間のベースライン時点でのright temporoparietal cortexの糖代謝低下により，overlapなしにconverterとnon-converterを区別することができたが，posterior cingulateはconverterとnon-converterでoverlapがあったと，比較的少数の症例数で報告されている．その後，Hiraoら[5]は，MCI converter，non-converter，健常対照群の間でECD脳血流SPECTを比較している．Converterは健常者と比較してprecuneusとposterior cingulate，inferior parietal，angular gyrus，parahippocampal gyrus，middle temporal gyrusで血流低下が認められたが，non-converterと比較した場合，inferior parietal，angular gyrus，precuneusでの低下が違いであったという．Posterior cingulateは，non-converter群でも健常者と比べて低下しており，むしろprecuneusがpredictorであった，と詳細な検討結果を報告している．

これらの報告に対して，posterior cingulate cortexも弁別上，重要であったとする結果もある．Drzezgaら[4]は，1年の縦断研究において，converter群では健常群と比較した場合temporoparietal cortex，posterior cingulate cortexでの糖代謝が低下しているが，non-converter群と比較した場合，最も大きな相違点はposterior cingulate cortexの低下であると報告している．Anchisiら[11]によると，amnestic MCI converterが健常群に比べて糖代謝が低下しているのは，inferior parietal，posterior cingulateで，加えてhippocampal/parahippocampal gyrusであり，non-converterと比較してもtemporoparietal metabolic patternであったという．Borroniら[2]は，ECD脳血流SPECT画像に対して，多変量解析により関心領域を設定した方法では，parietal，temporal，precuneus，posterior cingulate cortexを含む関心領域が，converterとnon-converterをよく鑑別できたとしている．

また，考慮すべき要因として，ADのリスクファクターであるアポリポタンパクE（apolipoprotein E；ApoE）ε4遺伝子がある．ApoE ε4遺伝子のキャリアーは，症状がない段階[10]，さらには若年者の段階[11]から，脳糖代謝がposterior cingulate～precuneus，parietotemporal association cortexで低下しており，AD的安静時神経活動のパターンを示すことが知られている．Mosconiら[8]がMCIに関して，ApoE遺伝子型と脳糖代謝低下パターンの関係を調べたところ，すべてのconverterは健常者と比べてinferior parietal cortexで糖代謝が低下していた．MCI患者でもε4遺伝子carrierは，ε4 non-carrierと比較すると，temporoparietal，posterior cingulate cortexで糖代謝低下が認められたという．

さらに，posterior cingulateの糖代謝低下は，50歳以上の健常者の約5%で認められることが知られている．このなかにADの病態をもつものが含まれることが十分考えられるが，他方変性性認知症の病態をもたない健常の加齢性変化の可能性もある．また，高齢発症のアルツハイマー型認知症では，脳血流/糖代謝低下は小さい傾向にあり，posterior cingulate～precuneusの血流/糖代謝低下は認められないこともある[12]．

このように，posterior cingulate cortexの脳血流/糖代謝（神経活動）は，遺伝子型，ADの病態，年齢などさまざまな要因で修飾される可能性があり，意義づけに関してはさらなる検討が必要であろう．

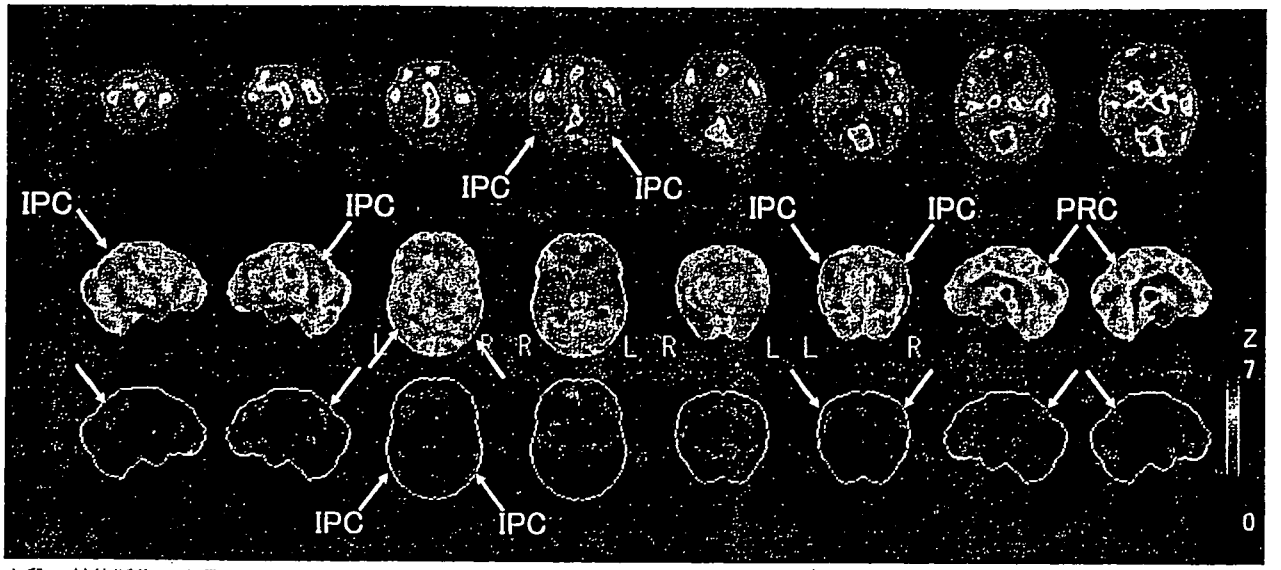

上段；軸位断像，中段；3D-SSP 脳血流投影像，下段；3D-SSP Z スコア画像
IPC ; inferior parietal cortex, PRC ; precuneus
アルツハイマー・パターンの軽微な脳血流低下が，下部頭頂葉（IPC），楔前部（PRC）に認められる．

図 3　MCI converter（rapid converter）症例の MCI 時点での [I-123] IMP 脳血流像

4 統計学的画像解析による脳血流 / 糖代謝画像の評価

脳血流 / 糖代謝画像による認知症診断でなくてはならないのが，SPM（statistical parametric mapping）や 3D-SSP（three-dimensional stereotactic surface projection）など統計学的画像解析の方法である．解剖学的標準化を行うことにより個人間で異なる脳の形状をあわせこみ，脳の全領域を対象に画素単位での統計比較を行い，結果である t 値や Z 値を画像として表示する．これにより，病態によってどの部位に低下があるかを明らかにするための群間比較や，健常者データベースとの比較による個人脳における血流 / 代謝低下部位の検出を行い診断に役立てる．

MCI においては，血流 / 糖代謝低下が非常に微弱であることがある．それでも inferior parietal cortex での低下は，primary motor-sensory area とのコントラストから，断層画像の視覚評価でも可能なことが多い．しかし，posterior cingulate ～ precuneus での軽微な脳血流 / 糖代謝低下は，評価がむずかしいことがある．それは，同域は，正常安静時，高血流 / 高代謝部位であり，その軽度の低下を視覚的に評価することは，容易ではないからである．このような場合でも，統計学的画像解析は画像の差異を鋭敏に検出することができる．

群間比較による低下部位の検出と患者個々における低下部位の検出では，様相をやや異にする．群間比較の場合，その低下の大きさ（変化率）が小さくても低下の傾向が系統的であれば，大きな統計値となって現れやすい．しかし，個々の脳，とくに MCI の患者を対象とする場合，健常者データベースの分散に比べて血流 / 糖代謝低下が十分大きくなく，統計画像上明瞭に現れない可能性がある．

図 3 は，converter 症例の MCI 時の [I-123] IMP 脳血流 SPECT 軸位断像と 3D-SSP 処理による脳表への脳血流投影像，その Z スコア画像である．微弱ながら下部頭頂葉，楔前部に血流低下が存在することがわかる．AD 的血流低下パターンであると診断することができる．図 4 は，MCI の non-converter の症例で，大脳に血流低下を示す部位は認められるものの軽微かつまばらであり，アルツハイマー的血流低下パターンは認められない．

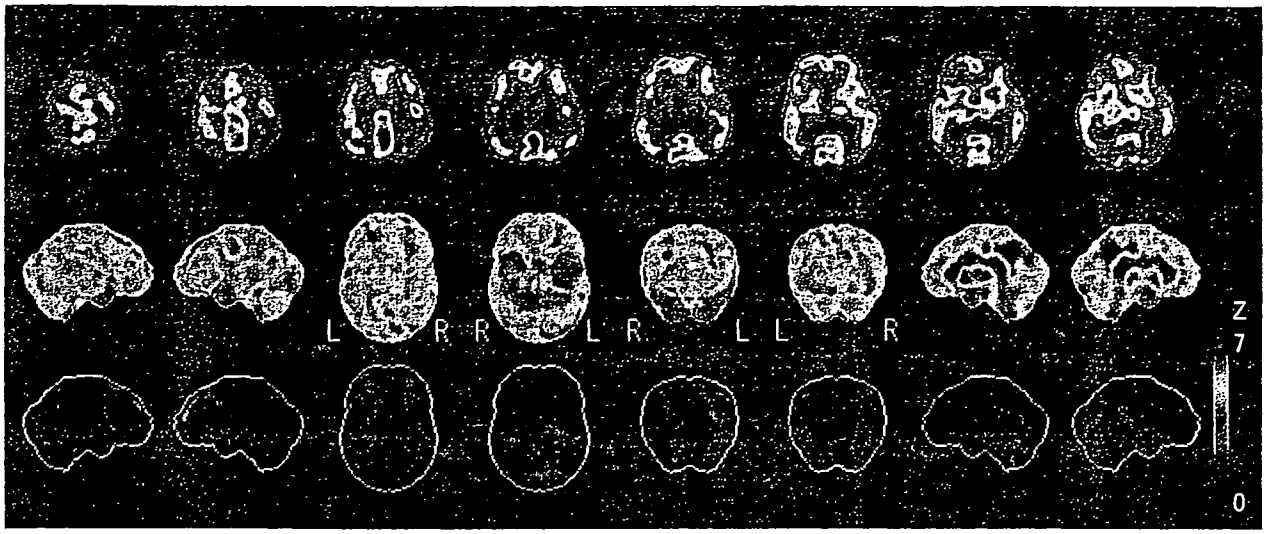

上段；軸位断像，中段；3D-SSP脳血流投影像，下段；3D-SSP Zスコア画像
アルツハイマー・パターンの血流低下は認められない．

図4　MCI non-converter（stable）症例の[I-123] IMP脳血流像

5 MCIを対象とする臨床試験としての多施設研究

現在MCIを対象に，画像検査の有効性を検証する大規模臨床研究が日本，ヨーロッパ，アメリカ合衆国，オーストラリアで行われている．

日本におけるJ-COSMIC（Japan Cooperative SPECT Study on Assessment of Mild Impairment of Cognitive Function）は，「MCIを対象としたアルツハイマー型認知症の早期診断に関する研究」で，財団法人・長寿科学振興財団の指定研究として平成15年度から実施されている．全国41施設が参加して，認知症の早期診断における脳血流SPECTの有用性を示すエビデンスを出すことを目標としている．

また，「MCIを対象とするADの早期診断に関する多施設共同研究（SEAD-Japan，Study on Diagnosis of early Alzheimer's disease-Japanの略）」は，厚生労働科学研究費補助金の援助を受けた多施設共同研究である．全国約10の医療機関で，MCI患者を対象として，認知症の早期診断におけるFDG-PET検査およびMRI検査，神経心理検査の有用性に関するエビデンスを示すことを目的としている．平成17年11月から始まった．

アメリカにおいては，ADNI（Alzheimer's Disease Neuroimaging Initiative）が，2005年7月に始まった．MCIだけでなく，AD，健常者を対象に含め総数800例のデータを全米で集める．全例に対してMRIを実施するほか，オプションとして糖代謝PET，アミロイドイメージング，遺伝子などの検査を実施する包括的かつ大型のプロジェクトである．

これらの研究プロジェクトは，MCIに関しては，いずれもADへの進行を予測する脳血流あるいは脳糖代謝変化の所見をより高いエビデンスレベルで確立するとともに，方法の標準化などを目指している．

こういった一連の研究は，ADの病態解明や早期診断を単に可能にするだけではなく，今後ワクチン療法などAD治療が可能になったときに，治療を開始する群の選別，治療効果のモニタリングなどを実施していく際に求められるさまざまな医学的エビデンスを提供することが期待されている．

文　献

1）Anchisi D, Borroni B, Franceschi M, Kerrouche N,

et al.: Heterogeneity of brain glucose metabolism in mild cognitive impairment and clinical progression to Alzheimer disease. *Arch Neurol*, 62 : 1728-1733 (2005).
2) Borroni B, Anchisi D, Paghera B, Vicini B, et al.: Combined 99mTc-ECD SPECT and neuropsychological studies in MCI for the assessment of conversion to AD. *Neurobiol Aging*, 27 : 24-31 (2006).
3) Chetelat G, Desgranges B, de la Sayette V, Viader F, et al.: Mild cognitive impairment ; Can FDG-PET predict who is to rapidly convert to Alzheimer's disease? *Neurology*, 60 : 1374-1377 (2003).
4) Drzezga A, Lautenschlager N, Siebner H, Riemenschneider M, et al.: Cerebral metabolic changes accompanying conversion of mild cognitive impairment into Alzheimer's disease ; A PET follow-up study. *Eur J Nucl Med Mol Imaging*, 30 : 1104-1113 (2003).
5) Hirao K, Ohnishi T, Hirata Y, Yamashita F, et al.: The prediction of rapid conversion to Alzheimer's disease in mild cognitive impairment using regional cerebral blood flow SPECT. *Neuroimage*, 28 : 1014-1021 (2005).
6) http://www.adni-info.org/images/stories/Documentation/adni_protocol_03.02.2005_ss.pdf
7) Ingelsson M, Fukumoto H, Newell KL, Growdon JH, et al.: Early Abeta accumulation and progressive synaptic loss, gliosis, and tangle formation in AD brain. *Neurology*, 62 : 925-931 (2004).
8) Mosconi L, Perani D, Sorbi S, Herholz K, et al.: MCI conversion to dementia and the APOE genotype ; A prediction study with FDG-PET. *Neurology*, 63 : 2332-2340 (2004).
9) Petersen RC, Smith GE, Waring SC, Ivnik RJ, et al.: Mild cognitive impairment ; Clinical characterization and outcome. *Arch Neurol*, 56 : 303-308 (1999).
10) Reiman RM, Caselli RJ, Yun LS, Chen K, et al. : Preclinical evidence of Alzheimer's disease in persons homozygous for the epsilon 4 allele for apolipoprotein E. *N Engl J Med*, 334 : 752-758 (1996).
11) Reiman RM, Chen K, Alexander GE, Bandy D, et al.: Functional brain abnormalities in young adults at genetic risk for late-onset Alzheimer's dementia. *PNAS*, 101 : 284-289 (2004).
12) Sakamoto S.: Differences in cerebral metabolic impairment between early and late onset types of Alzheimer's disease. *J Neurol Sci*, 200 : 27-32 (2002).